Int. J. Heat Mass Transfer. Vol. 20, pp. 1161–1172. Pergamon Press 1977. Printed in Great Britain

ANALYSIS OF THERMAL AND ELECTRICAL ENERGY TRANSPORT IN POCO AXM-5Q1 GRAPHITE

MERRILL L. MINGES
Air Force Materials Laboratory, Dayton, Ohio, U.S.A.

(*Received* 7 *September* 1976 *and in revised form* 7 *January* 1977)

Abstract—Thermal conductivity, thermal diffusivity, thermal expansion, electrical resistivity and heat capacity results which collectively encompass temperatures from 4 K to over 3000 K are presented on this graphite which is being considered as an international reference standard. Invoking the semi-continuum model for thermal energy transport, a theoretically predicted thermal conductivity curve is developed from 70 to 1000 K including crystal boundary and phonon–phonon scattering components. Graphite crystallite dimensions, the porosity/tortuosity factor and the modeling of crystallite interactions are shown to be fully reconcilable with theory and yield a predicted conductivity in very good agreement with the extensive measurements results. Above 1000 K and extending to 3000 K the experimental results from many different investigators show a clear hyperbolic temperature dependence in accord with expectations for a pure phonon conductor. Deficiencies in the theoretical modeling of energy transport in graphite are cited, and are shown to be relatively unimportant in the analysis conducted here.

A quantitative relationship between electrical conductivity and the crystal boundary limited component of the thermal conductivity over a wide temperature range is demonstrated. However, as expected, no general relationship was found between electrical conductivity and the total thermal conductivity. A series of recommendations are made for additional experimental measurements on this graphite.

NOMENCLATURE

C_n, constants, $n = 1$–6;
C_p, heat capacity [J/kg K];
e, electronic charge [e.m.u.];
$J_n(X)$, transport integral;
L, graphite crystallite scattering length or equivalent mean free path [Å];
Lo, Lorenz number [V^2/K^2];
n, carrier density [m^{-3}];
T, temperature [K].

Greek symbols

α, tortuosity/porosity factor ($=\beta\varepsilon$);
β, porosity/density factor;
ε, tortuosity factor;
θ, Debye temperature [K];
λ, thermal conductivity [W/m·K];
μ, carrier mobility [e.m.u.–s/kg];
ρ, electrical resistivity [Ω·m]; density [kg/m^3];
σ, electrical conductivity [$(\Omega\cdot m)^{-1}$];
τ, shear stress [$m^2 s^2$].

Subscripts

a, parallel to basal plane;
B, crystal boundary component;
c, perpendicular to basal plane;
e, electronic;
h, holes;
l, lattice;
L, longitudinal;
o, out-of-plane;
T, transverse;
TH, thermal;
u, Umklapp process or anharmonic 3-phonon interaction component;
1, longitudinal basal plane component;
2, transverse basal plane component;
3, out-of-plane basal plane component;
4. longitudinal c-axis component;
5, transverse c-axis component;
6, out-of-plane c-axis component.

1. INTRODUCTION

A RELATIVELY wide range of experimental electrical and thermal transport property measurement results on Poco AXM-5Q1 graphite* have become available recently because of its consideration for use as a broad temperature range international standard reference material for thermophysical properties. The comprehensive extent of the data base motivated this critical analysis of the empirical results based on theoretical interpretations of energy transport in graphite. These models have also been broadened and refined recently to the extent that quantitative, theoretically based expressions for the transport properties can be formulated without severely limiting assumptions at least above about 100 K which is the focus of this analysis.

The theoretical models deal with highly oriented, essentially defect- and void-free materials such as pyrolytic graphite. Thus, application of the correlations to polycrystalline materials such as this Poco graphite requires the use of essentially empirical

* Product of Poco Graphite, Inc., Garland, Texas. Grade designation: *AXM*: medium grain fuel cell grade; 5*Q*: 2500°C graphitization temperature; *1*: purified.

factors accounting for increased resistance to energy transport from the following effects: (a) variable orientation of the highly anisotropic graphite crystallites; (b) macro- and micro-voids; (c) intercrystalline contact resistance. Effect (a) is often termed the tortuosity factor, ε, while effects (b) and (c) are usually lumped as a density effect factor, β. Even though these effects may increase the resistance to thermal and electrical energy transport by over a factor of 10 above the levels observed for high quality pyrolytic graphite, it is generally found that the theoretically predicted temperature functionality of the transport properties is maintained. Support for this assertion is based at least in part of the fact that below the peak in the thermal conductivity curve (typically around 300 K for polycrystalline materials) but above temperatures where electronic contributions are important ($\sim$10 K) the temperature dependence of the thermal conductivity of polycrystalline graphites agrees with that observed for highly oriented pyrolytic graphite ($\sim T^{2.7}$) which in turn is reconcilable with recently refined theory. The tortuosity/porosity factor developed in analyzing thermal energy transport is also assumed to apply to correlation of electrical energy transport although there are some qualitative reasons to expect differences as elaborated on further below.

A further simplification of considerable significance is usually invoked in modeling energy transport in polycrystalline graphites. The basic graphite crystallites are very highly anisotropic, whether the material is single crystal, pyrolytically deposited or polycrystalline. The basal plane thermal conductivity is often over 200 times the c-axis conductivity [1, 2], whereas the electrical conductivity anisotropy ratio may even be greater, on the order of 1000 [3]. Thus, it is usually assumed that basal plane transport overwhelmingly dominates total transport in polycrystalline materials, and thus equations based on the theory parallel to the basal plane (that is, perpendicular to the hexagonal axis) are used to model net energy transfer. Most of the complications which limit the utility of the theory in its present state of development either arise at temperatures below about 50 K or have to do with the equations for the c-axis conductivity which will not be used here because the contribution of this component in polycrystalline graphite is so small. These effects have to do with (1) uncertainties in the elastic constant values used in evaluating the c-axis conductivity component and (2) sensitivity of the low temperature c-axis conductivity (below 50 K) to crystal boundary parameters (L_c is usually assumed to be infinite) and electronic contributions [4, 5]. The following analysis is confined to temperatures above 50 K using modeling results expressed in terms of the basal plane component only. Thus, the limitations of the theory of crystal boundary scattering fortunately are not especially important here.

In addition to the issue of allowing for finite values of L_c if indeed it is very small, on the order of $0.1L_a$ or less, Kelly and Taylor state that the other outstanding problem in the understanding of the thermal conductivity of graphite is possible electron contributions at temperatures above 2000 K [8]. As will be shown later no evidence of such contributions appears in the available results on AXM-5Q1.

2. THE SEMI-CONTINUUM MODEL OF CRYSTAL BOUNDARY SCATTERING

Above 10 K and extending to around 300 K crystal boundary scattering dominates thermal energy transport. Above 300 K and extending to at least 1000 K crystal boundary effects diminish gradually to negligible proportions as anharmonic phonon–phonon interactions assert dominance. Thus, the accurate modeling of crystal boundary scattering is most important over the range where the net thermal conductivity of graphite is changing rapidly and dramatically. Crystal boundary scattering of phonons has been most readily analyzed in quantitative terms using the relaxation time approximation and frequency spectrum equations based on the Komatsu semi-continuum model of dynamic lattice response. This model is based on the fact that there is strong interatomic bonding within the graphite basal plane but relatively weak binding between the layers. Thus, it is envisioned that the dynamic vibrational response of the lattice can be approximated as a system of elastically coupled thin plates. Each elastic plate responds to bending, stretching and shearing while adjacent plates couple via shear and tensile–compressive displacements [6]. Geometrically, the crystal boundary scattering of these thin plates is characterized by scattering lengths L_a and L_c perpendicular to the hexagonal axis (parallel to the basal plane) and parallel to the hexagonal axis (perpendicular to the basal plane), respectively.

Since the graphite crystal possesses hexagonal symmetry there are two independent principal thermal conductivities, λ_a and λ_c, respectively, parallel and perpendicular to the basal planes. The three acoustic modes. contributing to each of the principal conductivities are the in-plane longitudinal and transverse modes and the out-of-plane mode. Thus, the overall crystal boundary scattering limited conductivity can be represented as,

$$\lambda_B = \lambda_a + \lambda_c = \underbrace{[\lambda_1 + \lambda_2 + \lambda_3]}_{\substack{\text{basal plane} \\ \text{components}}} + \underbrace{[\lambda_4 + \lambda_5 + \lambda_6]}_{\substack{c\text{-axis} \\ \text{components}}}. \qquad (1)$$

If, as mentioned above, the contributions of the c-axis components to the total conductivity are neglected then the net crystal boundary limited conductivity becomes

$$\lambda_B \cong \lambda_a = \lambda_1 + \lambda_2 + \lambda_3. \qquad (1a)$$

In the quantitative calculations of each of these terms using the semi-continuum model further simplifications can be made. As a first approximation, for the longitudinal and transverse conductivity contributions parallel to the basal planes, λ_1 and λ_2, effects of the L_c boundaries are neglected (i.e. $L_c = \infty$); that is, scattering is assumed to be by the boundaries per-

pendicular to the basal plane only. The shear interaction between the layers is also neglected (i.e. $\tau = 0$). Under these conditions the in-plane modes λ_1 and λ_2 are essentially two-dimensional. For the out-of-plane model, λ_3, however (even with $\tau = 0$), significant velocity components exist parallel to each of the three principal axes and, hence, it is necessary to examine the extent to which finite values of L_c effect the magnitude of λ_3. The numerical calculations show that λ_3 is significantly effected when $L_c < 0.1\, L_a$ at low temperatures (below 100 K) but to a much lesser degree at higher temperatures [4].

The integral equations for λ_1, λ_2 and λ_3 developed by Kelly [4] and by Taylor *et al.* [7] are of the following form,

$$\lambda_1(T) = C_1 L_a J_3\left\{\frac{\theta_L}{T}\right\}\left[\frac{T}{\theta_L}\right]^2 \tag{2}$$

$$\lambda_2(T) = C_2 L_a J_3\left\{\frac{\theta_T}{T}\right\}\left[\frac{T}{\theta_T}\right]^2 \tag{3}$$

$$\lambda_3(T) = C_3 L_a\left[\frac{h}{kT}\right]^2\left[\frac{T}{\theta_o}\right]^2 J_{5/2}\left\{\frac{\theta_o}{T}\right\}. \tag{4}$$

An important point to note is the linear dependency of each component on the effective crystallite size L_a. Numerical evaluation of these equations and comparison with experimental results on pyrolytic graphite leads to the following general observations. First, the magnitudes of λ_1, λ_2 and λ_3 are such that, as shown in Table 1, each of the three acoustic modes contributes significantly to the total basal plane conductivity, λ_a. Second, for the two in-plane modes, assuming a zero value for the interplanar shear constant becomes questionable only below about 50 K; assuming $\tau = 0$ and $L_c = \infty$ is justified above these temperatures. Third, for the out-of-plane contribution to the basal plane conductivity, λ_3, assuming an infinite value of L_c does not effect the results. Only if $L_c \leqslant 0.1\, L_a$ does an effect arise and even this is of little importance at temperatures above about 100 K. Further, non-zero values of interplanar shearing are of little importance above 50 K for this component.

In summary, based on quantitative numerical results using the semi-continuum model, above 50 K little inaccuracy is introduced in assuming that $L_c = \infty$ and $\tau = 0$ in the equations for the total conductivity of graphite parallel to the basal planes. Further, the crystallite boundaries parallel to the hexagonal axis define an effective basal plane scattering length L_a. This scattering length is equivalent to an effective crystallite size for the basal plane "thin plates". Since λ_1, λ_2 and λ_3 are directly proportional to L_a the value assumed for this important independent physical variable is most significant in the temperature range where crystal boundary scattering dominates the total conductivity. In the analysis which follows, a value of $L_a = 1500$ Å was applied based on two considerations:

(a) According to data of Klein and Taylor [6], for an annealing temperature of 2500°C (which is used for AXM-5Q1), the mean free path for crystal boundary scattering is in the 1000 Å range.

(b) Correlations of thermal conductivity measurements for polycrystalline graphites by Taylor [7] yield L_a values in the 1500–2000 Å range.

The significance of the value of the crystallite size used in arriving at an analytical expression for the total thermal conductivity begins to diminish as the temperature moves above 300 K since the crystal boundary limited conduction contribution to the total conductivity gradually decreases. At around 1000 K the influences are small since anharmonic three-phonon scattering is the principal determinant of the effective scattering mean free path and in turn of the effective total conductivity.

The numerical values for λ_1, λ_2 and λ_3 calculated by Kelly [4] and by Taylor *et al.* [7] do not agree exactly. Discussion with the authors [29] indicated that a small numerical error existed in the Taylor *et al.* results and thus the data of Kelly should be used. The latter was therefore applied in the calculation of λ_a for AXM-5Q1 graphite.

3. THE THERMAL CONDUCTIVITY IN THE 70–1000 K RANGE

In this temperature range, encompassing the peak in the conductivity curve, both crystal boundary scattering and anharmonic phonon interactions contribute significantly to the total effective conductivity. Below the peak in the curve, from approximately 70–300 K, crystal boundary scattering predominates. Beyond the peak the anharmonic phonon interaction component is increasingly dominant. Quantitatively the thermal resistivities are presumed to be additive as indicated in equation (5). Further, as mentioned above, it is assumed that the basal plane conduction λ_a dominates the total conduction and that the tortuosity/porosity

Table 1. Relative contributions of the three components of the crystal boundary limited thermal conductivity of graphite

Temperature T (°K)	Longitudinal component $100\lambda_1/\lambda_a$ (%)	Transverse component $100\lambda_2/\lambda_a$ (%)	Out-of-plane component $100\lambda_3/\lambda_a$ (%)
100	18	27	55
200	21	29	50
400	32	30	38
600	38	30	32
800	41	29	30
1000	42	28	30

Table 2. Crystal boundary and anharmonic phonon scattering contributions to the total thermal conductivity of AXM-5Q1 graphite ($\alpha = 7.17$)

Temperature T (°K)	Total conductivity λ (W/m·K)	Crystal boundary component $100\lambda_B/\lambda$ (%)	Umklapp process component $100\lambda_u/\lambda$ (%)
70	12.3	99.8	0.2
100	25.1	99.5	0.5
150	51.1	98.2	1.8
200	75.3	89.7	10.3
250	88.7	76.4	23.6
300	95.7	65.7	34.3
400	90.1	45.8	54.2
500	83.5	35.3	64.7
600	78.5	29.8	70.2
800	67.4	22.2	77.8
1000	58.0	18.3	81.7

correction required to express the transport in polycrystalline materials in terms of the expressions developed for well ordered graphites is encompassed in the factor $\alpha = \varepsilon\beta$,

$$\lambda^{-1} = \alpha\lambda_a^{-1} = \alpha[\lambda_B^{-1} + \lambda_u^{-1}]. \quad (5)$$

With the model described in the previous section along with the restriction discussed (principally $\tau = 0$, $L_c = \infty$, $L_a = 1500$ Å) the theoretically predicted crystal boundary scattering component λ_B for AXM-5Q1 can be derived.

The quantitative relationship for λ_u as a function of temperature was an exponential of the form $\lambda_u \propto e^{\theta/T}$, where $\theta = 2480$ K is an average value Debye temperature suggested by Taylor [2]. Unfortunately, the theoretical basis for the modeling of phonon–phonon interaction conduction in graphite which predominates at high temperatures is developed in only a rudimentary form. Thus, the calculations of λ_u are really empirically based. As discussed later there is a rationale for assuming that the anharmonic phonon interaction component of the total thermal resistivity is simply linear in temperature, $\lambda_u \alpha T^{-1}$, which gives a better overall representation of the empirical measurement results as the temperature is extended above 1000 K.

The results of the calculations are plotted in Fig. 1 and tabulated in Table 2. Table 2 also includes the relative contributions of λ_B and λ_u as a function of temperature. At 100 K over 99% of the total conduction is due to crystal boundary effects. In the vicinity of the peak, just below 300 K, λ_B and λ_u are comparable in magnitude. At 1000 K over 80% of the total is due to anharmonic phonon interaction contributions. The numerical values in the second column of Table 2 represented the theoretically predicted total thermal conductivity of AXM-5Q1 graphite. Unfortunately, experimental results are not available below 300 K, and hence experimental confirmation of the position of the peak and the overall shape of the curve is yet to be established.

Experimental data, both directly measured thermal conductivity and conductivity inferred from measured thermal diffusivity, is available above 300 K. A comparison of the predictions from theory and the experimental measurements along with the λ_B and λ_u components are shown in Fig. 1. The experimental results curves are least squares fits of an extensive series of thermal conductivity (upper curve) and thermal diffusivity (lower curve) measurements by different investigators on AXM-5Q1 graphite [9]. The actual experimental data points are shown in Figs. 2 and 3 in thermal resistivity form.

The value of the empirical tortuosity/density correction factor, α, was determined by matching the theoretically predicted conductivity at 1000 K ($\lambda = 416.0$) with the least squares fit of the experimental direct conductivity results ($\lambda = 58.0$). Thus, $\alpha = 416.0/58.0 = 7.17$. This value compares favorably with an average value of $\alpha = 7.53$ for a series of polycrystalline graphites analyzed by Taylor *et al.* [7], although the spread of their values ($\alpha = 4.25$–13.9) was rather wide since highly anisotropic polycrystalline graphites unlike the Poco material were included.

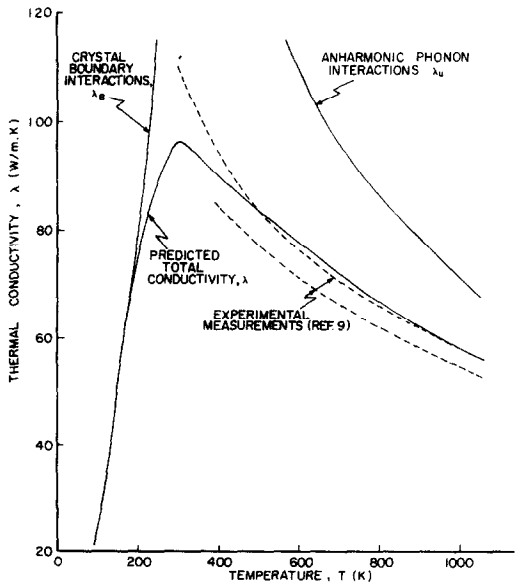

FIG. 1. Predicted and measured thermal conductivity of Poco AXM-5Q1 graphite.

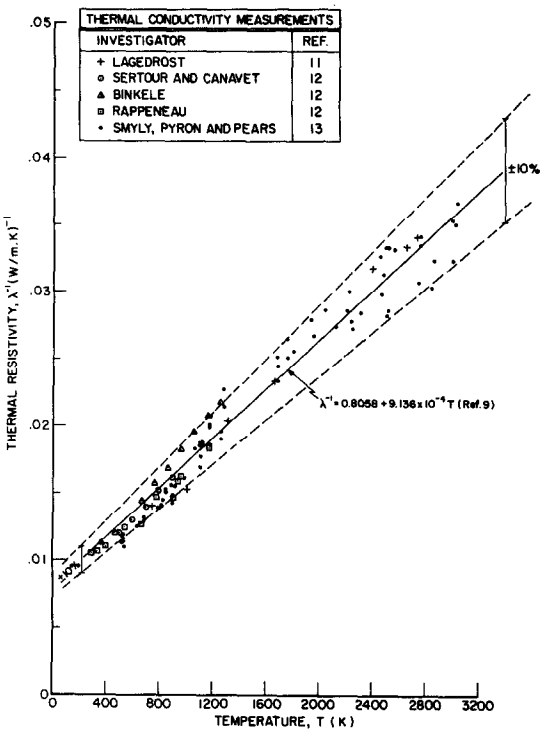

FIG. 2. Thermal conductivity measurement results plotted as $\lambda^{-1} = f(T)$.

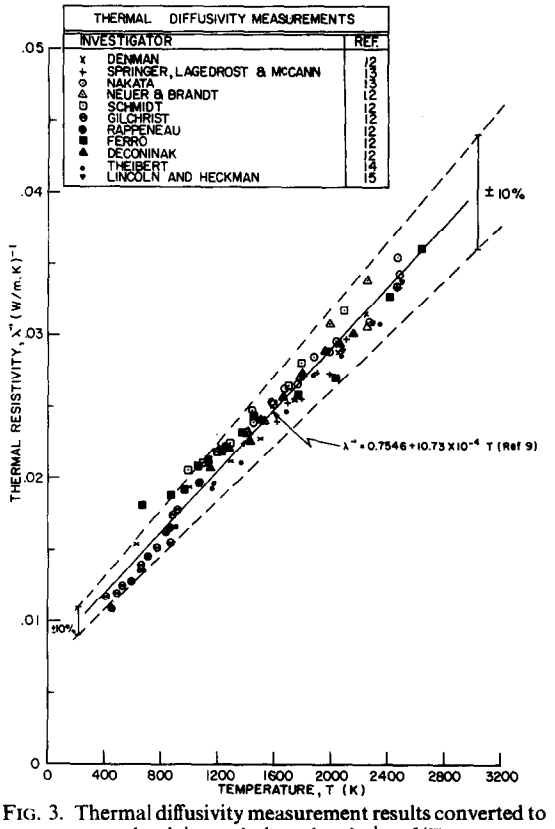

FIG. 3. Thermal diffusivity measurement results converted to conductivity and plotted as $\lambda^{-1} = f(T)$.

For isotropic graphites presumably more clearly analogous to AXM-5Q1 the range was somewhat narrower ($\alpha = 5.3$–7.15).

The location of the peak in the predicted total conductivity curve is sensitive to the value of L_a both with respect to the temperature at which it occurs and the absolute magnitude of the thermal conductivity. Higher values of L_a both increase the magnitude of the maximum conductivity and decrease the temperature at which the maximum occurs. Higher values of L_a correspond to a more ordered structure which could be affected by higher annealing temperatures, for example. However, the value of L_a chosen does not much affect the calculated value of α since in the case discussed here α was purposely calculated at 1000 K where the crystal boundary contribution is relatively small, around 18% according to Table 2.

4. ANHARMONIC PHONON INTERACTION LIMITED CONDUCTIVITY: 1000–3000 K

As the temperature increases beyond the maximum in the conductivity curve, predicted to occur around 300 K for this graphite, the contribution of phonon–phonon limited conduction becomes predominant; at 1000 K this component contributes over 80% as mentioned earlier and completely dominates the total conduction at higher temperatures unless mechanisms such as ambipolar diffusion or other phenomena of basic electronic origin come into play. As will be shown below, the measurement results on this graphite do not substantiate the existence of any electronic contribution even at the highest test temperature, 3000 K.

As pointed out by Kelly [6, 10], no comprehensive theory of phonon–phonon scattering in the anisotropic graphite crystal lattice has yet been developed, so quantitatively predicted values of polycrystalline graphite conductivity at high temperatures are not traceable to first order principles. Numerical predictions are thus derived from classical analyses of the temperature functionality predicted for ordered dielectrics with the various numerical constants involved being evaluated via curve fitting of experimental data. An expression of this form was used in the previous section in describing the phonon–phonon scattering contribution up to 1000 K. There is a difference of opinion as to whether the temperature functionality of the anharmonic phonon conductivity is exponential or hyperbolic. Kelly [10] notes that the conductivity above the peak falls roughly exponentially at first and then at a decreasing rate up to about 2000 K. Confirming the exponential dependence at temperatures up to 900 K with pyrolytic graphite data, Taylor [2] notes a linear relationship between $\ln(\lambda_a)$ and T^{-1}. It is further suggested that above 2000 K the conductivity becomes temperature independent, a phenomenon of electronic origin. The results on AXM-5Q1 graphite show disagreement with these observations to the extent that both the direct conductivity results and the thermal diffusivity results (converted to conductivity) show a temperature dependence following a T^{-1} relationship from 400 K all the way to 3000 K. However, below 1000 K deviation from linearity is expected since the crystal boundary limited component is significant. Figures 2 and 3 present the thermal transport property measurement results from a considerable number of in-

vestigations in Europe and the United States using a variety of measurement techniques, both steady state and transient. Altogether 16 different sets of measurements are included. Although most of the results are summarized in [9], in Figs. 2 and 3 the primary literature sources are cited where numerical data can be found. Within the spread of the measurement results plotted in thermal resistivity form in these figures, no functionality other than linear is really justified, although polynomial fits can also be applied to the data (Table 4 [9]). This dependence does not, however, conflict with Taylor's suggestion of an exponential dependence in the 400–900 K range since either a hyperbolic or an exponential temperature functionality represents the data within the scatter of the numerical results over this limited range.

Logatchov and Skal [16] have outlined in rudimentary form a theoretical treatment of phonon–phonon scattering basal plane thermal conductivity suggesting that the in-plane modes dominate the conduction at high temperatures. It is concluded that a thermal resistivity linear in temperature is to be expected outside the region where crystal boundary scattering contributes.

The thermal resistivity curves from Figs. 2 and 3 are replotted in Fig. 4 along with the theoretically predicted total conductivity curve from Fig. 1 (as λ^{-1}). A

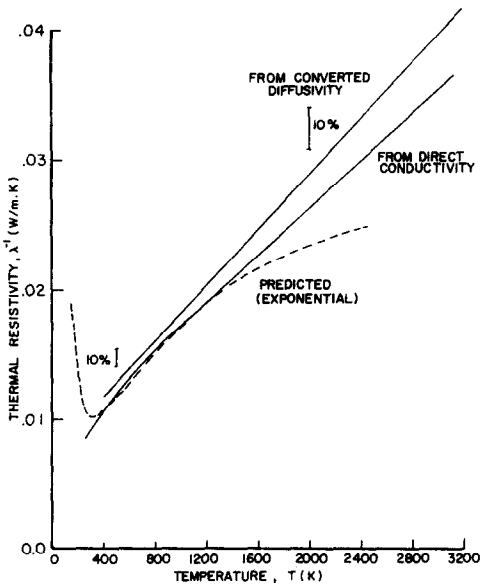

FIG. 4. Thermal resistivity: comparison of theory and experiment.

nonlinear term has been included in the direct conductivity curve below 1000 K since it produces a better fit with the experimental data. The deviation of the predicted conductivity from the linear representation of the experimental data below about 800 K is expected since crystal boundary scattering contributions become important as the temperature decreases. The agreement of the direct conductivity experimental results and the theoretical predictions of combined crystal boundary/phonon–phonon scattering, equations (2)–(5), was found to be excellent between 300 and 1000 K as displayed in Fig. 1.

Looking to temperatures above 1000 K, it is interesting to note in Fig. 4 that even up to about 1600 K the exponential temperature dependence for phonon–phonon scattering used in the predicted relationship gives essentially the same results as a linear thermal resistivity. At temperatures above 1600 K, however, the exponential thermal resistivity dependence dips rapidly below the actual measurement results which follow a linear dependence as shown in Figs. 2 and 3.

The differences between the two linear thermal resistivity relationships in Fig. 4 describing the directly measured thermal conductivity and the conductivity derived from measured diffusivity represent an anomaly which is not presently resolvable. Even with the spread in the numerous measurement results the approximate 5% difference in the least squares curves at high temperature is considered to be real, representing most likely systematic measurement errors rather than uncertainties in density–heat capacity data used in the diffusivity conversion.

The density and heat capacity results used to convert the measured diffusivity to thermal conductivity are shown in Fig. 5 where a thermal expansion correction for the density has been applied. The thermal expansion coefficient used (Table 6 [17]) was derived from direct measurements on this material [18, 19] and is estimated to have an uncertainty of no more than 4%; thus, the temperature corrected density is considered to be accurate to better than 1%, the main uncertainty being the inaccuracy in the baseline room temperature density rather than its variation with temperature which is estimated to be known within 0.5%. The uncertainties in heat capacity especially at higher temperatures are estimated to be about 3% based on the direct measurements on this graphite by Cezairliyan and Righini [20] and the agreement of these results with the data of West and Ishihara [21] (within 0.6%) using an entirely different measurement technique. Representative numerical C_p data points are shown in Fig. 5 including the lower temperature measurements of Binkele [12] also made on this Poco graphite. At lower temperatures (below 1400 K) a curve fitting the results of Binkele was used since the equation of West and Ishihara was valid only above this range.

5. ELECTRICAL ENERGY TRANSPORT IN AXM-5Q1 GRAPHITE

(A) *Thermal and crystal boundary scattering*

A series of electrical resistivity measurements on AXM-5Q1 graphite by Cezairliyan and Righini [20] and Hust [22] have broadened the temperature range coverage on this property so that the curve can be estimated from 4 K all the way to 3000 K. These results together with the measurements previously reported by Brandstaedter and Binkele [12] are shown in Fig. 6. The $\rho(T)$ relationship was established by drawing a

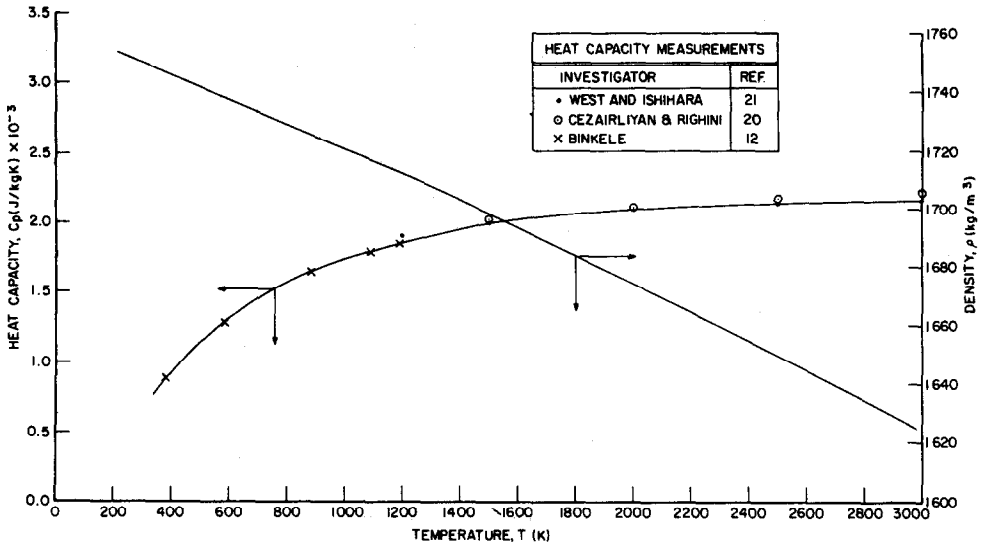

FIG. 5. AXM-5Q1 Poco graphite heat capacity and density.

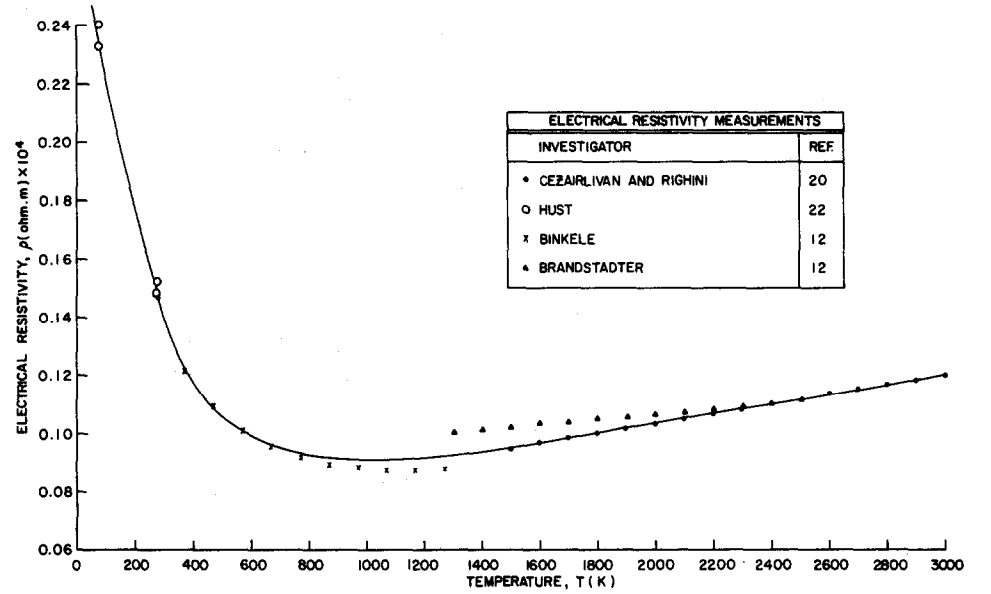

FIG. 6. AXM-5Q1 Poco graphite electrical resistivity.

curve directly through the high temperature data of Cezairliyan and Righini and through the low temperature data points of Hust. In the mid-temperature range the curve is a good representation of the average Binkele/Brandstaedter results although individually these measurements deviate from the curve by about 5–8%. Because of these differences an average uncertainty in electrical resistivity is difficult to specify although at the high temperature end Cezairliyan and Righini estimate their error to be only 1%. At and below room temperature the resistivity is apparently quite sensitive to specimen–specimen variations with an interspecimen spread of up to 10% according to Hust [22]. However, individual measurements by Hust were found to be accurate to within 1% or better.

With these electrical transport property results and the thermal transport property information from the previous section, it is possible to examine in quantitative terms the relationships between these transport mechanisms. As with thermal transport it is envisioned that the electrical resistivity of a polycrystalline graphite is that of the in-plane component (perpendicular to the c-axis) of the single crystals multiplied by an empirical factor accounting for density–tortuosity effects [3]. The same empirical factor as that derived for thermal transport, $\alpha = \varepsilon\beta$, is often invoked [7].

The functional form of the theoretically based expression for the electrical conductivity is written as the electronic charge multiplied by the product of the mobility and carrier density for holes and electrons. If an average carrier mobility $\bar{\mu} = (\mu_e \mu_h)^{1/2}$ is assumed along with an average temperature dependent carrier density, a relatively simple expression results. The reciprocal of the average mobility is further expanded

in terms of a mean free path with crystal boundary and thermal scattering components. Thus,

$$\rho = \rho_a \alpha = \alpha[e(\mu_e n_e + \mu_h n_h)]^{-1} \simeq \alpha[n_e + n_h]^{-1}[e\bar{\mu}]^{-1}$$
$$\simeq \alpha[(n_e + n_h]^{-1} C_4 \left[\frac{1}{L_a} + \frac{1}{L_{TH}}\right]$$
$$\simeq \alpha[C_4/(C_5 + C_6 T)]\left[\frac{1}{L_a} + \frac{1}{L_{TH}}\right]. \quad (6)$$

Even though there is an apparent general empirical relationship between electrical and thermal conductivity of polycrystalline graphites around room temperature [23–26] there is no reason to expect a general proportionality between electrical conductivity and total thermal conductivity over a wide temperature range for at least two important reasons: (1) unless temperatures are extremely low (~10 K) or extremely high (above 2500–3000 K) no significant amount of net thermal energy is transported via electrons, (2) phonon–phonon scattering which does not involve electrons at all contributes significantly to the total thermal resistance at all temperatures above about 100 K. The lack of any such simple relationship is seen in the insert, Fig. 7, where electrical conductivity is plotted as a function of total thermal conductivity. The relationship is not even single value. Just for reference, the various empirical relationships between the room temperature electrical and thermal transport quoted in the literature [23–25] give thermal conductivities predicted based on experimental electrical resistivity values for AXM-5Q1 between $\lambda = 93.0$ and $\lambda = 98.0$ (W/m·K) about 30% below the experimental results (Figs. 1–3). Thus, these apparently general relationships do not hold for Poco AXM-5Q1 graphite.

On the other hand if it is assumed that crystal boundary scattering is the predominant influence on electrical conductivity, then a proportionality could be anticipated between the electrical conductivity and the crystal boundary scattering component of the thermal conductivity. Such a relationship was indeed found to exist for Poco graphite between about 70 and 700 K as shown in Fig. 7.

Equation (6) can be used to calculate the mean crystallite size, L_a, based solely on electrical transport measurements. This avenue of approach provides a method of independently cross-checking the value of L_a calculated from the thermal transport property correlations. Applying equation (6), the value of L_a was calculated using low temperature electrical resistivity data (where L_{TH} was large and hence L_{TH}^{-1} was small). Calculated values of L_a were 957 and 1233 Å at 77 and 273 K respectively.

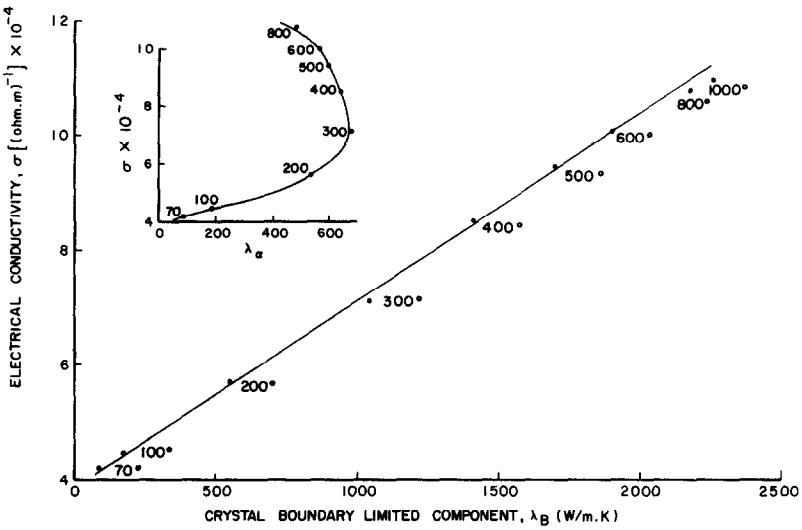

FIG. 7. Correlation between electrical conductivity and crystal boundary limited thermal conductivity.

These values are in the same range as the values assumed in the thermal conductivity correlation but somewhat lower in numerical value: 36 and 18% respectively. Other investigators found L_a values calculated from electrical resistivity data to be in general agreement with values deduced from the thermal properties although the scatter in the results amounted to over 100% (cf. Fig. 24, [6]). Taylor *et al.* [7] found that L_a values obtained from electrical data were from 30 to 50% lower than those obtained from thermal conductivity analysis on a series of polycrystalline graphites. Their results are thus consistent with the calculations above for AXM-5Q1 graphite. Reasons offered for these observed differences include (1) different values of α may govern thermal and electrical transport; for example, contact resistance effects may act differently in impeding thermal and electrical energy transport, (2) a significant influence of defects on electron/hole carrier concentrations, (3) crystallite orientation influences electrical transport to a greater degree than thermal transport giving net lower values of L_a for electrical transport.

(B) *Electronic contributions to thermal energy transport*

A mechanistically superficial yet widely used index for evaluating whether there is a significant electron contribution to thermal energy transport is the magnitude and temperature dependency of the Wiedmann–Franz ratio: the measured thermal conductivity times the measured electrical resistivity divided by the temperature, $\lambda\rho/T$. This function divided by the classical Sommerfeld free electron gas value of the Lorenz function, Lo, is plotted in Fig. 8. If this ratio is significantly above unity then it is said that lattice conduction predominates. From Fig. 8 it is clear that this situation obtains with the ratio even exceeding 400 around 150 K. Even in the 2000–3000 K range the Wiedmann–Franz ratio is several times Lo and is still a strong function of temperature.

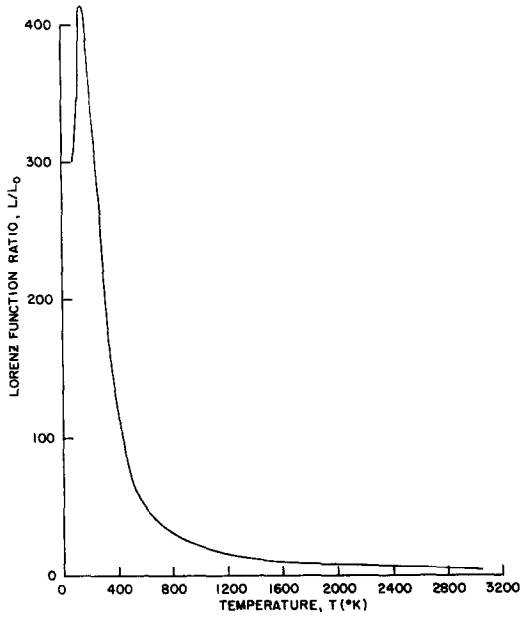

FIG. 8. Wiedmann–Franz/Lorenz function ratios as a function of temperature for AXM-5Q1 Poco graphite.

At a temperature of about 2000 K the Wiedmann–Franz ratio is about nine times Lo. This fact coupled with the linear dependence of the thermal resistivity with temperature discussed earlier strongly suggests that electronic contributions to net thermal energy transport are insignificant.

In the range between 2000 and 3000 K a further examination of the measurement results is required in evaluating possible electronic effects on the thermal conductivity. As observed elsewhere [9], two basically different approaches are generally used. The first is to assume that the total thermal conductivity is given by $\lambda = \lambda_e + \lambda_l$ and thus that the electronic contribution is the difference between the measured total conductivity and the lattice conductivity. If the lattice component is assumed to obey a $\lambda_l^{-1}\alpha T$ functionality (usually extrapolated from low temperatures), then the numerical values of the "predicted" electronic component is simply the difference of $\lambda - \lambda_l$. The second approach is to develop a theoretically based expression for the Lorenz function and in turn the electronic contribution to thermal energy transport based on some assumed mechanism of energetic electron interaction. Then the difference between the measured total conductivity and the "predicted" electronic component, $\lambda - \lambda_e$, at high temperature is attributed to either lattice conduction (αT^{-1}) and/or to inaccuracies in the assumed transport model.

The first approach is illustrated in an analysis of transport property measurements on ATJ-S and a different, finer grain Poco graphite (AXF-5Q) by Bapat and Nickel [26, 27]. These authors conclude for both these graphites that the electronic contribution increases from a very low level at 1000 K (5% or less) to about 20–25% in the 3000–3300 K range. The effective Lorenz ratio which follows from this analysis was on the order of Lo. The difficulty with this approach, which is not discussed by these authors and in turn a factor which weakens the assertion of significant high temperature electronic contributions, is the uncertainty in the inferred electronic contribution which arises due to the scatter in the measured total thermal conductivity, λ. Since the electronic component is calculated as the difference between the measured conductivity λ and a lattice component, $\lambda_l = (T^{-1}), \lambda_e = \lambda - \lambda_l$, then any imprecisions in λ will be greatly magnified in the value of λ_e especially if the difference $\lambda - \lambda_l$ is small. Thus, if the inaccuracy of the measured conductivity, λ, is in the range of $\pm 10\%$ which is typical for such materials at high temperatures ($\pm 7\%$ is quoted by these authors) a substantial uncertainty is introduced in deriving an effective electronic component which is claimed to contribute only 5–25% of the total. It is a question of inferring small differences between relatively large numbers where there is a significant error band associated with the latter. Further, since the effective Lorenz ratio is calculated from the inferred electronic contribution via the Wiedmann–Franz ratio a similar large uncertainty in its magnitude also occurs. Thus, even though there is a trend in the results given by these authors for the measured total high temperature thermal conductivity to lie above a $\lambda\alpha T^{-1}$ curve extrapolated from low temperatures, it is not entirely clear that the difference can be ascribed to electronic effects at least to the quantitative degree suggested. Other measurements on the ATJ-S graphite by Lincoln and Heckman [15] show a somewhat lower total measured conductivity in the 2000–3500 K range than that obtained by Bapat although some additional uncertainty may have been introduced in converting the Lincoln/Heckman measured diffusivity results to thermal conductivity. However, the Lincoln/Heckman results on the ATJ-S graphite are such that no electronic component whatever need be introduced to explain the temperature dependency in the 2000–3500 K range.

For the measurement results on AXM-5Q1 graphite presented earlier in Figs. 2 and 3, the spread in the data are such that it simply is not warranted to assume anything other than a $\lambda\alpha T^{-1}$ functionality. Further,

no trend away from this temperature dependency is noted in the 2000–3000 K range. Thus, based on this analysis approach, the results are fully reconcilable with the pure lattice conduction model. In the long run though, higher accuracy thermal measurements will be vital to resolve clearly these different interpretations as to the presence or absence of relatively small high temperature electronic contributions.

The second analysis approach requires (1) the statement of an electron energy transport model, (2) the calculation of an effective Lorenz function as a logical consequence of this model and (3) the calculation of an electronic contribution to thermal transport using the Lorenz function and measured electrical resistivity in a Wiedmann–Franz Law relationship. The more recently developed models of describing high temperature contributions of electronic origin which could be invoked in this approach are reviewed by Kelly and Taylor [8]. Briefly, it is expected that a constant Wiedmann–Franz ratio above 2000 K is a natural consequence of significant bipolar contributions to the net thermal energy transport. The bipolar contributions are then modeled in terms of either the simple two-band model or a true energy band model. Quantitative evaluations based on these models give effective Lorenze number from 2 to 3 times the classical value, Lo. Assessing the electrical and thermal property measurement results on AXM-5Q1 using this model the following observations were made: (1) between 2000 and 3000 K, with $L = Lo$ the inferred lattice component of the thermal resistivity, $(\lambda - \lambda_e)^{-1}$ exhibits a linear temperature dependency, (2) between 2000 and 3000 K, with $L = 3Lo$, $(\lambda - \lambda_e)^{-1}$ deviates up to about 22% from temperature linearity, (3) with the higher value of the Lorenz function L = 3L o, the calculated electronic component at 2500 K is about 50%.

Unlike the conclusions using the first analysis approach the above observations using the second approach are inconclusive as to the presence or absence of a significant electronic component. With $L = Lo$ the first observation is consistent with the conclusion that there is an electronic component increasing from about 12–22% between 2000 and 3000 K. On the other hand, bipolar modeling suggests higher values of L and dominent electronic conduction by the time 2500 K is reached. With $L = 3Lo$ the nonlinearity and large magnitude of the inferred lattice component (the second and third observation above) are inconsistent with expectations.

6. CONCLUDING REMARKS

Intrinsic features which make Poco ASM-5Q1 graphite very attractive as a standard reference material include its ease of machining, low cost, extreme temperature range coverage, diffuse surface texture, high emittance and tenaceous physical stability with proper graphitization. Factors to be explored more fully in the context of reference material suitability are intra and interlot variability of density, electrical resistivity and the proper quantitative indices needed to assure that a given specimen or lot of material is truly homogeneous relative to the transport properties, especially the thermal transport properties. Further, it is necessary to establish whether the sensitivity of the transport properties to the homogeneity indices is a function of temperature. For example, small variations in density and/or electrical resistivity near room temperature may be directly reflected in interspecimen variations of the thermal conductivity, whereas at 1500 K for example, those effects may no longer be important. Hust has found that the LHe, LN_2 and ice point electrical resistivities both intra and interlot can be quite variable, on the order of 10% [22]. Once the density effect variations are separated out it is necessary to establish whether electrical resistivity variations are a sensitive index of the main property of interest—thermal transport. There is reason to suspect, based on the analyses of the foregoing sections, that electrical resistivity variability may not be of great significance as an index of thermal transport homogeneity of a given lot of specimens or lot of graphite material. Density will clearly be important, and specimens in the range of 1750 kg/m^3 can readily be selected using conventional measurement approaches or such techniques as radiation gaging [28].

As regards the experimental measurement data base on AXM-5Q1 graphite, the results displayed earlier are most encouraging considering the large number and diversity of measurements conducted. However, several areas deserve further exploration including the following:

(1) Thermal transport property measurements below 300 K, down to at least 70 K, preferably 4 K to confirm or refute the predicted low temperature conductivity curve presented in Fig. 1 and Table 2. Simultaneous evaluation of specimen density and electrical resistivity should be conducted to establish the magnitude and importance of the thermal/electrical transport and density relationship in the range around room temperature and below.

(2) Measurement of the effective graphite crystallite size independent of its inference from electrical and/or thermal transport correlation equations would be of utmost importance in quantitatively predicting the crystal boundary scattering limited component of the total thermal conductivity.

(3) More extensive electrical resistivity evaluations are required in the mid-temperature range from around room temperature to about 1500 K to decrease the mid-temperature range uncertainty of this property. Results reconcilable within 2–3% are not unreasonable to expect.

(4) As stated elsewhere [9], higher precision, higher accuracy thermal conductivity measurements (on the order of ±1%/±3% respectively) should be relatively straightforward with this material up to around 1200 K. At present the imprecision is at least on the order of 10% (Figs. 5 and 7 [17]). These more accurate empirical results will allow confirming the hyperbolic phonon–phonon conduction relationship extrapolatable to higher temperatures. The improvement in

this quantitative relationship would in turn allow (a) exploration of the apparently real systematic differences between measured conductivity and converted thermal diffusivity and (b) the issue of very high temperature electronic contributions to thermal energy transport.

The analysis approach used here can be applied to other graphites where sufficient characterization information is available. The primary literature on these materials can be accessed readily through [30].

REFERENCES

1. M. R. Null, W. W. Lozier and A. W. Moore, Thermal diffusivity and thermal conductivity of pyrolytic graphite from 300 to 2700 K, *Carbon* **11**, 81–87 (1973).
2. R. Taylor, The thermal conductivity of pyrolytic graphite, *Phil. Mag.* **13**, 157–166 (1966).
3. G. H. Kinchin, The electrical properties of graphite, *Proc. R. Soc.* **A217**, 9–20 (1953).
4. B. T. Kelly, Theory of the effect of crystallite boundaries on the principal thermal conductivities of highly oriented graphite, *Carbon* **6**, 71–80 (1968).
5. B. T. Kelly, Theory of the effect of crystallite boundaries on the principal thermal conductivities of highly oriented graphite—the effect of the elastic constant C_{44}, *Carbon* **6**, 485–496 (1968).
6. B. T. Kelly, The thermal conductivity of graphite, *Chem. Phys. Carbon* **5**, 119–215 (1969).
7. R. Taylor, K. E. Gilchrist and L. J. Poston, Thermal conductivity of polycrystalline graphite, *Carbon* **6**, 537–544 (1968).
8. B. T. Kelly and R. Taylor, The thermal properties of graphite, *Chem. Phys. Carbon* **10**, 1–140 (1973).
9. M. L. Minges, Evaluation of selected refractories as high temperature thermophysical property calibration materials, *Int. J. Heat Mass Transfer* **17**, 1365–1383 (1974).
10. B. T. Kelly, Present understanding of the thermal properties of graphite, *High Temp.—High Pressures* **5**, 133–144 (1973).
11. J. F. Lagedrost, Personal Communication, Battelle Memorial Institute (30 January 1969).
12. E. Fitzer, Thermophysical properties of solid materials at high temperatures, Project Section II: cooperative measurements on heat transport phenomena of solid materials at high temperature, AGARD Advisory Report R-606 (1973).
13. A. Wechsler, R. Carroll, C. Costas, P. Doherty, P. Glaser and S. Gray, Development of high temperature thermal conductivity standards, Air Force Materials Laboratory Technical Report 69-2 (1969).
14. L. S. Theibert, Personal Communication, Air Force Materials Laboratory (22 January 1976).
15. R. C. Lincoln and R. C. Heckman, Negative-pulse thermal diffusivity measurements of ATJ-S graphite to 3500 K, *High Temp.—High Pressures* **7**, 71–77 (1975).
16. Y. A. Logatchov and A. S. Skal, On the theory of basal plane thermal conductivity of graphite, *Carbon* **9**, 711–714 (1971).
17. M. L. Minges, Evaluation of selected refractories as high temperature thermophysical property calibration materials, *Rev. High Temp. Materials* **II** (4), 305–371 (1975); also Air Force Materials Laboratory Technical Report TR-74-96 (1975).
18. E. Fitzer, Thermophysical properties of solid materials, Project Section 1A: Cooperative thermal expansion measurements up to 1000°C, AGARD Advisory Report 31 (1971).
19. E. Fitzer, Thermophysical properties of solid materials, Project Section 1B: Thermal expansion measurements from 1000 to 2600°C. AGARD Advisory Report 38 (1972).
20. A. Cezairliyan and F. Righini, Measurements of heat capacity, electrical resistivity and hemispherical total emittance of two grades of graphite in the range 1500 to 3000 K by a pulse heating technique, *Rev. Int. Htes. Temp. of Refract.* **12** (2), 124–131 (1975).
21. E. D. West and S. Ishihara, A calorimetric determination of the enthalpy of graphite from 1200 to 2600 K, in *Advances in Thermophysical Properties at Extreme Temperature and Pressure*, pp. 146–151. ASME, New York (1965).
22. J. G. Hust, Personal Communication, National Bureau of Standards (January 1976).
23. C. Y. Ho, R. W. Powell and P. E. Liley, Thermal conductivity of selected materials, NSRDS-NBS 16 (1968).
24. D. L. McElroy, T. E. Kellie, W. M. Ewing, R. S. Graves and R. M. Steele, Room temperature measurements of electrical resistivity and thermal conductivity of various graphites, Oak Ridge National Laboratory TM-3477 (1971).
25. J. P. Moore, R. S. Graves and D. L. McElroy, Thermal and electrical conductivities and seebeck coefficients of unirradiated and irradiated graphites from 300 to 1000 K, *Nucl. Technol.* **22**, 88–93 (1974).
26. S. G. Bapat and H. Nickel, Thermal conductivity and electrical resistivity of Poco Grade AXF-Q1 graphite to 3300 K, *Carbon* **11**, 323–327 (1973).
27. S. G. Bapat, Thermal conductivity and electrical resistivity of two types of ATJ-S graphite to 3500 K, *Carbon* **11**, 511–514 (1973).
28. G. E. Lockyer, Investigation of nondestructive methods for the evaluation of graphite materials, Air Force Materials Laboratory Technical Report TR-65-113 (1965).
29. R. Taylor, Personal Communication, University of Manchester, England (May 1976).
30. C. Y. Ho, R. W. Powell and P. E. Liley, Thermal conductivity of the elements: a comprehensive review, *J. Phys. Chem. Ref. Data* **3**, Suppl. 1 (1974).

ANALYSE DU TRANSFERT DES ENERGIES THERMIQUE ET ELECTRIQUE DANS LE GRAPHITE POCO AXM-5Q1

Résumé—On présente, pour ce graphite qui est considéré comme un étalon international de référence, des résultats sur la diffusivité thermique, la dilatation thermique, la résistivité électrique et la capacité thermique entre 4 et 3000 K. A partir d'un modèle semi-infini pour le transfert d'énergie thermique, on donne une courbe théorique entre 70 et 1000 K, incluant la frontière du cristal et la diffusion phonon-phonon. Les dimensions du cristal de graphite, le facteur de porosité/tortuosité et la modélisation des intéractions de cristallites sont pris en compte par la théorie et conduisent à une conductivité en très bon accord avec les résultats expérimentaux. Au dessus de 1000 K et jusqu'à 3000 K, différents résultats expérimentaux montrent clairement une dépendance hyperbolique vis à vis de la température, en accord avec l'hypothèse d'un pur conducteur à phonons. On énumère les faiblesses de la modélisation théorique du transfert d'énergie dans le graphite et on montre qu'elles sont relativement sans importance dans l'analyse faite ici.

On donne une expression quantitative entre la conductivité électrique et la composante, limitée par la frontière du cristal, de la conductivité thermique, dans un large domaine de température. Néanmoins aucune relation n'a été trouvée entre la conductivité électrique et la conductivité thermique totale. On formule une série de recommandations pour les mesures additionnelles sur ce graphite.

UNTERSUCHUNG DES TRANSPORTS THERMISCHER UND ELEKTRISCHER ENERGIE IN POCO AXM-5Q1 GRAPHIT

Zusammenfassung—Für diesen Graphit, der als internationaler Referenzstandard betrachtet wird, werden Wärmeleitfähigkeit, Temperaturleitfähigkeit, thermischer Ausdehnungskoeffizient, elektrischer Widerstand und spezifische Wärmekapazität für Temperaturen von 4 K bis 3000 K angegeben. Aufgrund eines Halbkontinuum-Modells für den thermischen Energietransport wird die Wärmeleitfähigkeit zwischen 70 K und 1000 K berechnet, wobei die Gitter- und die Phononen-Streuungskomponenten berücksichtigt werden. Es wird gezeigt, daß die Graphit-Kristallabmessungen, der Porositäts- und Verwindungsfaktor und das Modell der gegenseitigen Kristalleinwirkungen vollständig mit der Theorie übereinstimmen; die errechneten Werte der Wärmeleitfähigkeit stimmen sehr gut mit den umfangreichen Meßwerten überein. Zwischen 1000 K und 3000 K zeigen die Meßwerte vieler verschiedener Autoren eine eindeutig hyperbolische Temperaturabhängigkeit, wie sie sich für einen reinen Phononenleiter erwarten läßt. Auf Fehler im theoretischen Modell für den Energietransport in Graphit wird hingewiesen; in der hier durchgeführten Untersuchung erweisen sie sich als relativ unbedeutend. Es wird ein quantitativer Zusammenhang zwischen der elektrischen Leitfähigkeit und der Gitterkomponente der Wärmeleitfähigkeit über einen weiten Temperaturbereich aufgezeigt. Erwartungsgemäß konnte jedoch kein allgemeiner Zusammenhang zwischen der elektrischen Leitfähigkeit und der gesamten Wärmeleitfähigkeit gefunden werden. Hinweise zur weiteren experimentellen Untersuchung dieses Graphits werden gegeben.

АНАЛИЗ ПЕРЕНОСА ТЕПЛОВОЙ И ЭЛЕКТРИЧЕСКОЙ ЭНЕРГИИ В ГРАФИТЕ POCO AXM-5QI

Аннотация — В работе представлены результаты комплексного исследования коэффициентов теплопроводности, температуропроводности, теплового расширения, удельного электрического сопротивления и теплоемкости в диапазоне температур от 4 К до свыше 3000 К для графита POCO AXM-5QI, который рассматривается как международный эталон. На основе теоретической квазиконтинуальной модели переноса тепловой энергии построена кривая теплопроводности для диапазона от 70 К до 1000 К с учетом рассеяния на поверхности кристалла и фонон-фононного рассеяния. Показано, что размеры графитового кристалла, коэффициент пористости-извилистости и моделирование взаимодействий кристалла полностью согласуются с теорией и позволяют получить хорошее соответствие между расчетными и измеренными значениями электропроводности. Экспериментальные результаты для диапазона температур свыше 1000 К и вплоть до 3000 К, полученные другими исследователями, показывают чёткую гиперболическую температурную зависимость, которая согласуется с теоретическими данными для чисто фононного проводника.

В статье отмечаются ограничения предложенной модели при рассмотрении переноса энергии в графите, но показано, что они не являются существенными в проводимом анализе. Показано количественное соотношение между электропроводностью и теплопроводностью поверхности кристалла в широком диапазоне температур. Однако, как и следовало ожидать, общей зависимости между электропроводностью и суммарной теплопроводностью обнаружено не было. Предложен ряд рекомендаций по проведению дополнительных экспериментальных измерений на графите.